PROCEEDINGS OF SCIENCE

Systematic uncertainties in radio emission of extensive air showers: A comparison of CoREAS and ZHAireS

Carlo S. Cruz Sanchez,[a] **Patricia M. Hansen,**[a] **Matias Tueros,**[a] **Jaime Alvarez-Muñiz**[b,*] **and Diego G. Melo**[c]

[a] *Instituto de Fisica La Plata, CONICET-UNLP, Diagonal 113 entre 63 y 64, La Plata, Argentina*
[b] *Instituto Galego de Física de Altas Enerxías, Univ. de Santiago, 15782 Santiago de Compostela, Spain*
[c] *ITeDA (CNEA - CONICET - UNSAM), CAC - CNEA; Av. Gral Paz 1499, San Martin - Buenos Aires, Argentina*

E-mail: jaime.alvarez@usc.es

Radio detection of extensive air showers induced by ultra-high energy cosmic rays has significantly advanced in recent decades. Observables such as shower energy and depth of maximum development are largely derived by comparing experimental data with Monte Carlo simulations, making it essential to assess the systematic uncertainties associated with the simulation models. In this work, we present a comprehensive comparison between CoREAS and ZHAireS, the two most widely used simulation codes for modeling radio emission from air showers. We simulated showers initiated by different primary particles, with various arrival directions and geomagnetic conditions, ensuring similar input parameters and the same altitude-dependent atmospheric refractive index in both cases. We find a good agreement between CoREAS and ZHAireS, with differences in the electric field components, across the MHz to hundreds of MHz frequency range, that are typically below 5% in the Cherenkov cone, the region where the electric field is stronger, and below 10% elsewhere. These differences result in uncertainties of $\simeq$ 10% on the energy released in the form of radio waves, and $\simeq 10\,\mathrm{g/cm^2}$ in the depth of shower maximum reconstruction due to the differences between the models.

39th International Cosmic Ray Conference (ICRC2025)
15 - 24 July 2025
Geneva, Switzerland

ICRC 2025
The Astroparticle Physics Conference
Geneva July 15-24, 2025

*Speaker

PoS(ICRC2025)174

1. Introduction.

Ultra-high-energy cosmic rays (UHECRs) initiate extensive air showers (EAS) upon entering the atmosphere. To investigate their nature and origin, several detection techniques are employed, including particle detectors, fluorescence telescopes, and radio antenna arrays. The radio technique, which detects MHz – GHz signals produced mainly by the geomagnetic and Askaryan effects, offers nearly continuous operation and reduced atmospheric attenuation. It enables accurate reconstruction of the primary energy [1] and the depth of maximum shower development ($X_{\rm max}$) [2, 3].

Reliable interpretation of radio data requires detailed simulations, mainly performed using the two state-of-the-art CoREAS and ZHAireS packages. These Monte Carlo tools calculate electric fields from first principles without assuming any emission mechanism. Previous comparisons between them have shown general consistency [4] but were limited in scope. This work extends and complements such comparisons by analyzing more fundamental observables such as the lateral distribution of electric field components and their frequency spectra, as well as the energy emitted in the form of radio waves. Additionally, we study the impact of the choice of simulation tool on radio-based $X_{\rm max}$ reconstruction. Further details on this work can be found in [5].

2. Monte Carlo Simulations of Radio Emission in EAS

Radio emission in EAS is modeled using Monte Carlo simulations where the electric field is obtained as the superposition of individual contributions from charged particles. The particle tracks are divided into small rectilinear sub-tracks under the assumption of constant velocity. The total electric field is calculated by summing the contributions of these sub-tracks in the time and/or frequency domains. This technique is employed in both CoREAS and ZHAireS.

CoREAS [6] is an extension of the CORSIKA [7] simulation package that computes radio emission using the *endpoints algorithm* [8]. In this approach, radiation is emitted at the discrete points where particle velocities change (accelerations or decelerations). CoREAS accounts for the altitude-dependent refractive index of the atmosphere $n(h)$, and for different atmospheric models, including the Gladstone-Dale law [9]. The CORSIKA 7.7410 and CoREAS v1.4 versions are employed here.

ZHAireS [10] simulates EAS using AIRES [11] to propagate particles, applying the *ZHS algorithm* [12] to compute radio emission. Similarly to the endpoints method, in the ZHS expression for the electric field, there are two terms for each sub-track corresponding to the start and the end points. However, the ZHS algorithm uses a fixed distance R to the observer for both points, whereas CoREAS calculates a separate R for each. This distinction becomes relevant for sub-tracks that are not short compared to R. Additionally, near the Cherenkov angle only the ZHS expression for the field yields a correct and finite limit, while the endpoints algorithm reverts to it. Simulations in this work were performed using AIRES 19.04.08 and the most recent version of ZHAireS 1.1.0a that includes the Gladstone-Dale model for $n(h)$.

To ensure a meaningful comparison, simulations were performed with matched settings for primary particle properties, threshold energies and other relevant parameters, as well as geometry, magnetic field, hadronic model, and refractive index. Identical kinetic energy thresholds were used for both simulations: 300 MeV for nuclei, 10 MeV for muons, and 250 keV for electrons

and gammas. To manage computational load, both codes implement thinning, and to reduce discrepancies, equivalent thinning levels and maximum weights were used. A CORSIKA parameter (STEPFC) adjusts the step size in electromagnetic tracking affecting the amplitude of radio emission. ZHAireS uses a fixed, finely stepped tracking scheme. STEPFC was set to 0.05 in CoREAS, close to the ZHAireS effective value [4] for consistency. Both programs now support modern LHC-tuned models and QGSJETII.04 [13] was adopted for consistency. Finally, both CoREAS and ZHAireS model $n(h)$ using the Gladstone-Dale law, with the refractive index proportional to atmospheric density, and in this work we use the same atmospheric model in both simulations.

A key element of this work is the use of a *controlled* shower selection procedure. A large number of air showers were first simulated with CORSIKA and AIRES (without radio emission), using identical primary type, energy E, and geometry (θ, φ) with the shower axis parallel to $\hat{v}$. From these, 20 showers were selected with $X_{\max}$ values within $1\,\mathrm{g/cm^2}$ of a chosen target value. These selected showers were then re-simulated with CoREAS and ZHAireS including radio emission, using identical geomagnetic field $\vec{B}$ settings and other relevant parameters. Since the inclusion of radio modules does not alter the random number sequence, the selected $X_{\max}$ values were preserved. This approach eliminates the need for corrections related to geomagnetic angle or atmospheric density at $X_{\max}$, reducing variations due to intrinsic shower fluctuations and allowing for a more direct and unbiased comparison of the radio signals produced by both codes.

3. Comparison of radio emission: CoREAS and ZHAireS

3.1 Electric field

Firstly we focus our analysis on the component of the electric field, parallel to the Lorentz force $\hat{v} \times \vec{B}$, denoted as E_y in the following. This component is mainly due to the geomagnetic mechanism and dominates for all the shower geometries and magnetic field configurations chosen in this work.

In the left panel of Fig. 1 we compare the lateral distribution of E_y as predicted by CoREAS and ZHAireS for iron-induced showers. The field is evaluated at 50 MHz as a function of the off-axis angle α/α_C, where α_C is the Cherenkov angle at the depth of shower maximum. The average $\langle E_y \rangle$ from a set of 20 simulations selected with $X_{\max}$ values within $1\,\mathrm{g/cm^2}$ of a target value are shown as well as the minimum and maximum values of E_y and the relative difference (ZHAireS – CoREAS)/ZHAireS between simulations. Both codes predict a similar lateral profile, featuring a clear *Cherenkov ring*, with two peaks in E_y close to α_C. Within the core region ($|\alpha/\alpha_C| \lesssim 1.5$), CoREAS and ZHAireS agree to within $\lesssim 5\%$, with ZHAireS consistently predicting slightly smaller E_y amplitudes. Differences grow at larger distances.

In the right panel of Fig. 1 the modulus of the Fourier component of E_y is shown as a function of frequency for two off-axis angles $\alpha = \alpha_C$ and $\alpha = 1.5\,\alpha_C$. For observers near the Cherenkov ring, E_y increases linearly below $\sim 5\,\mathrm{MHz}$, flattens in the range 5 – 100 MHz, and then declines beyond 100 MHz. This is consistent with coherence effects: at low frequencies, contributions from all shower particles add coherently; flattening occurs as time delays from shower front curvature and thickness introduce partial decoherence; and at high frequencies, increased time lags and lateral spread reduce coherence, steepening the spectrum [14]. Observers farther from the Cherenkov

ring see spectral suppression at lower frequencies due to destructive interference of different stages in shower longitudinal evolution. In the experimentally relevant 30 – 80 MHz band, ZHAireS consistently predicts electric fields $\lesssim$ 5% smaller than CoREAS. Below $\sim$ 10 MHz, ZHAireS amplitudes can slightly exceed CoREAS ones. At frequencies above 300 MHz, larger discrepancies emerge, exceeding a few percent.

The origin of the differences themselves remains unidentified. They may be due to minor variations in the energy loss model, the treatment of Coulomb multiple scattering, the tracking of electromagnetic particles, or the thinning algorithms, among other factors. A more detailed investigation, beyond the scope of this work, is required.

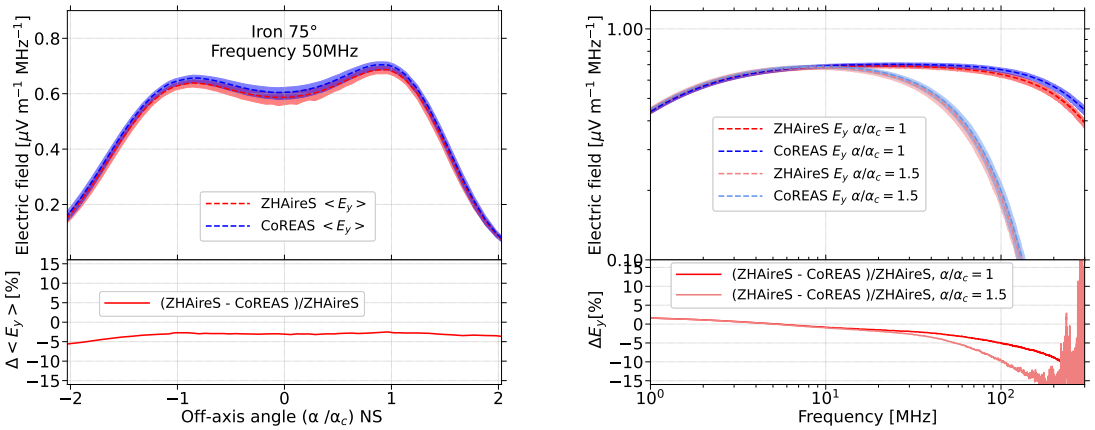

Figure 1: Modulus of the Fourier component E_y of the electric field from 20 simulations with ZHAireS and CoREAS, for iron primaries with $E = 10^{17}$ eV and $\theta = 75°$. All showers have $X_{\max}$ within 1 g/cm^2 of 574.5 g/cm^2. A vertical magnetic field of $|\vec{B}| = 50, \mu$T, pointing north and perpendicular to the ground, was used. Dashed lines show the average $\langle E_y \rangle$, and the shaded areas span from the minimum to the maximum E_y across the 20 simulations for ZHAireS (red) and CoREAS (blue). The bottom panel of each plot shows the relative difference between the averages, (ZHAireS – CoREAS)/ZHAireS. Left panel: E_y component at 50 MHz as a function of the off-axis angle α with respect to the Cherenkov angle α_C (see text). Right panel: Frequency spectrum of E_y for observers located at off-axis angles $\alpha/\alpha_C \simeq 1$ and $\alpha/\alpha_C \simeq 1.5$.

Fig. 2 summarizes the comparison between CoREAS and ZHAireS for the different primaries (proton, iron, and electron) and geometries ($\theta = 45°$ and $75°$) considered in this study. It shows the maximum value of E_y at 50 MHz as a function of the fraction of the primary energy carried by the electromagnetic component of the shower, which is expected to account for most of the radio emission. As anticipated, the signals are strongly correlated with the electromagnetic energy. An almost linear dependence of E_y on this fraction is observed for all primaries. Proton showers exhibit larger fluctuations than iron and also larger electromagnetic energy fraction, reflecting greater variability in their electromagnetic content. Electron-induced showers show higher electromagnetic energy and reduced spread, as expected. Overall, across all configurations and observer positions, ZHAireS systematically predicts slightly lower electric fields than CoREAS. At the reference frequency of 50 MHz, the difference is approximately 5%. For the same primary energy, $E_{y,\max}$ is higher at $\theta = 45°$ than at $\theta = 75°$, mainly due to the shorter distance to the ground observers.

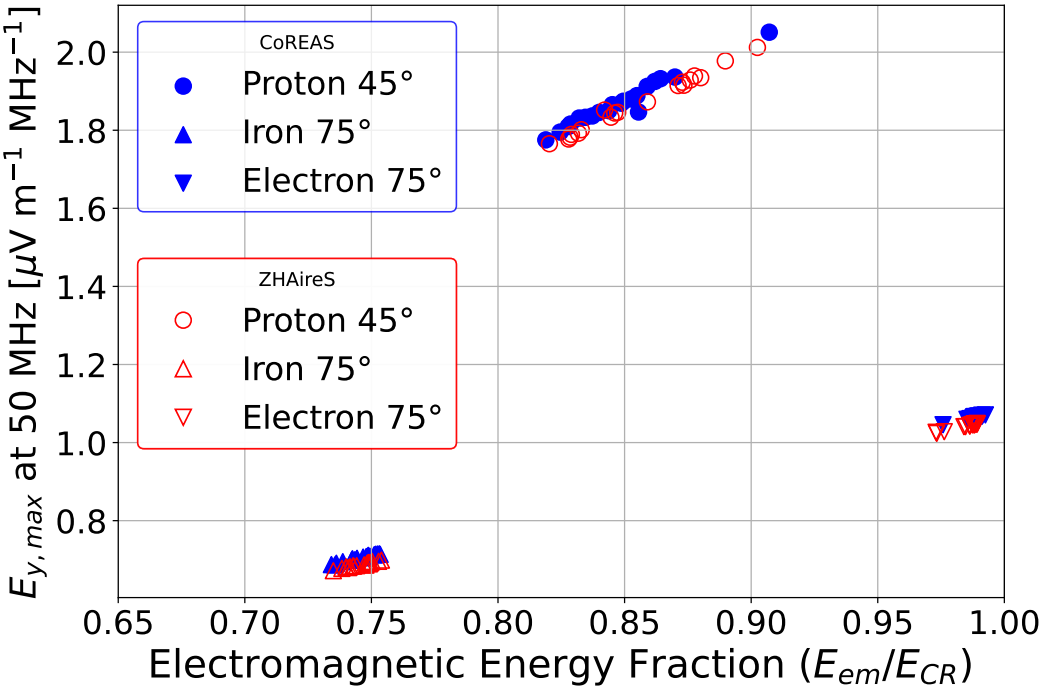

Figure 2: Peak value of the y-component of the electric field ($E_{y,\max}$) at 50 MHz versus the fraction of the primary energy carried by electromagnetic particles, for primary protons with $E_{CR} = 10^{17}$ eV at $\theta = 45°$ (circles), iron at $\theta = 75°$ (triangles), and electrons at $\theta = 75°$ (inverted triangles). Filled blue symbols represent CoREAS simulations; empty red symbols represent ZHAireS simulations.

3.2 Energy Radiated in Radio Waves

The energy radiated as radio waves in a given frequency band, often called *radiation energy*, is a robust estimator of the electromagnetic energy in air showers and, thus, correlates with the primary particle energy [1, 15]. Previous studies reported a $\sim 5.2\%$ higher radiation energy from CoREAS compared to ZHAireS in the 30 – 80 MHz band [4]. In Fig. 3 we present energy fluence maps for iron showers at $\theta = 75°$. Simulated events were selected to have nearly identical $X_{\max}$ values. The fluence maps, shown in the shower plane with axes aligned along $(\hat{v} \times \vec{B})$ and $\hat{v} \times (\hat{v} \times \vec{B})$, were interpolated from simulated antenna positions, with denser coverage near the core. The footprint is rather symmetric due to the relatively smaller Askaryan contribution compared to the enhanced geomagnetic effect in the lower-density atmosphere and larger geomagnetic angle at $\theta = 75°$. The relative difference in fluence between ZHAireS and CoREAS is within -10% for all positions on the shower plane. Integration over area yields a total average radiated energy of $\simeq 0.40$ MeV (CoREAS) and $\simeq 0.37$ MeV (ZHAireS), an -8% difference, consistent with the smaller values of electric field predicted by ZHAireS. These values are in agreement with measurements of radiation energy [1], yielding 0.64 ± 0.27 MeV after proper scaling for energy and geomagnetic angle. Across all cases studied in this work, ZHAireS systematically predicts lower radiation energy than CoREAS, with relative differences of $4 - 8\%$ depending on geometry and primary type.

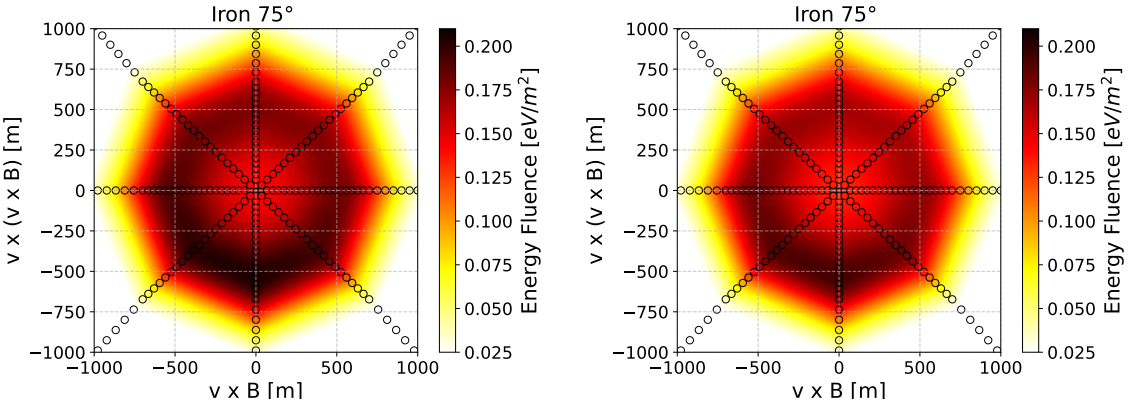

Figure 3: Maps of the radio energy fluence in the 30 – 80 MHz band (color scale) in the shower plane, averaged over 20 air showers simulated with CoREAS (left) and ZHAireS (right). Simulations are for an iron primary with $E = 10^{17}$ eV and $\theta = 75°$, with $X_{\max}$ values within 1 g/cm^2 of 574.5 g/cm^2, and a vertical field configuration with $|\vec{B}| = 50\,\mu$T, perpendicular to the ground. The x- and y-axes show distances along the $\hat{v} \times \vec{B}$ and $\hat{v} \times (\hat{v} \times \vec{B})$ directions, respectively.

3.3 Depth of shower maximum

Multiple methods have been developed to reconstruct $X_{\max}$ from radio data [16, 17], with the most precise results achieved by matching measured radio footprints to detailed air-shower simulations [16, 18]. This technique has successfully reconstructed $X_{\max}$ with a resolution better than $\sim 15\,\mathrm{g/cm^2}$ at energies around 10^{19} eV in measurements from AERA [3, 19], as well as from other experiments including Tunka-Rex [20], and LOFAR [2].

In this work, we adopt an overly simplified version of the reconstruction method in [16, 17]. Our focus is not on validating or further improving the reconstruction technique itself, but rather on quantifying the intrinsic uncertainty in $X_{\max}$ arising from the choice of simulation program needed to estimate $X_{\max}$. Therefore, we do not consider uncertainties associated with shower energy, geometry, or core position. We simulated 250 proton- and 250 iron-induced showers at $E = 10^{17}$ eV with $\theta = 45°$, using a magnetic field parallel to the ground with strength $|\vec{B}| = 50\,\mu$T pointing north. The simulations used a square antenna grid with spacing $D = 250$ m. The depth of maximum was allowed to vary freely across simulations to fully sample the $X_{\max}$ range. The reconstruction procedure involves selecting one of the 500 simulated showers as the *reference*, treated as mock data with known $X_{\max}^{\text{true}}$ while the remaining showers form the *reconstruction set*. This is done using both CoREAS and ZHAireS, and the roles of reference and reconstruction sets are alternated. Specifically, a single CoREAS shower is randomly chosen as the reference, and $X_{\max}$ is reconstructed using either the rest of the CoREAS set or the full ZHAireS set. The same is done using a ZHAireS shower as the reference. This allows direct comparison of $X_{\max}$ reconstruction within and between the two programs.

For each reference shower, we compute $\Delta^2 = \sum_{\text{i=antennas}} \left(u_i{}^{\text{ref}} - f_r^2\, u_i\right)^2$ with u_i the energy fluence in the antenna i in the event. Additionally, we have introduced a scaling factor f_r to account for possible differences in the overall amplitude of the electric field. A Δ^2 value is computed for each reference shower to identify the one in the reconstruction set with the smallest Δ^2 that provides the best match, with f_r optimized for each shower in the reconstruction set to yield the minimum

possible Δ^2. The corresponding depth of maximum, $X_{\rm max}^{\rm rec}$, is then taken as the reconstructed value. The simplicity of the method is intentional, avoiding complications from fit procedures, or detector response effects. This makes the comparison between CoREAS and ZHAireS simulations more transparent, isolating the influence of the simulation program on the reconstruction performance.

In the left panel of Figure 4 we show an example of the reconstruction process. Specifically, the reference shower to be reconstructed is induced by a proton simulated with ZHAireS and reconstructed with the reconstruction set of 500 CoREAS showers. Despite the simplified technique, the reconstructed $X_{\rm max}$ differs from the true value by less than $\sim 7\,{\rm g/cm^2}$.

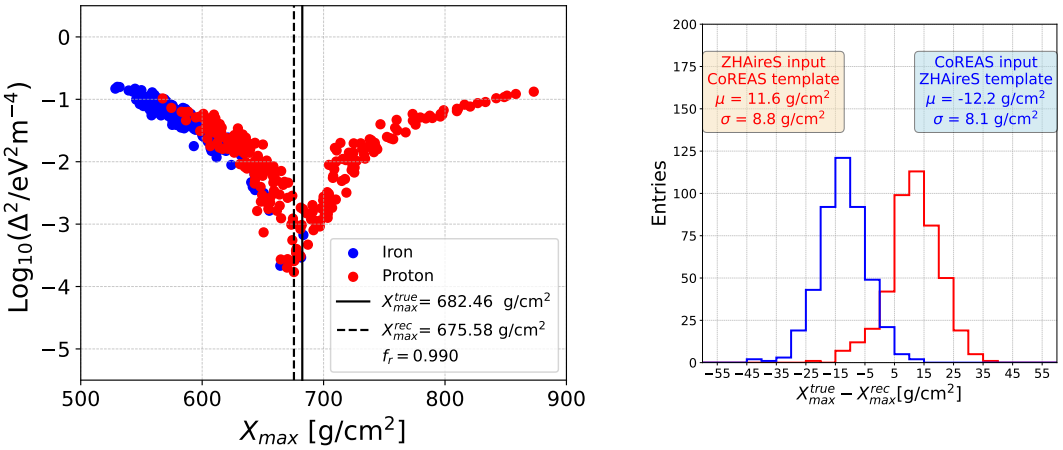

Figure 4: Left panel: Example of the methodology used to reconstruct $X_{\rm max}$, for a shower with $E = 10^{17}$ eV and $\theta = 45°$. In this case, the shower to be reconstructed is a proton simulated with ZHAireS and compared to 500 CoREAS showers (red: protons, blue: iron). The value of $\log_{10}(\Delta^2/{\rm eV}^2\, m^{-4})$ (see text) is plotted as a function of the simulated $X_{\rm max}$ of the ZHAireS showers. The true $X_{\rm max}^{\rm true}$ and reconstructed $X_{\rm max}^{\rm rec}$ are indicated by solid and dashed black lines, respectively. Right panel: Distribution of $[X_{\rm max}^{\rm true} - X_{\rm max}^{\rm rec}]$ (g/cm^2) for 450 reference proton and iron showers with $E = 10^{17}$ eV and $\theta = 45°$. Input and template showers are simulated with different codes.

To assess potential reconstruction biases in $X_{\rm max}$ within and across simulation programs, we repeated the reconstruction procedure using 450 randomly chosen p and Fe showers from each of the CoREAS and ZHAireS datasets. Each selected shower was treated as a reference and reconstructed using either template CoREAS or ZHAireS showers. When reconstruction is performed within the same simulation code, the mean value of the difference between the true and reconstructed values of $X_{\rm max}$ shows no significant bias, the σ values range from 5.9 to 7.4 g/cm^2, and $\langle f_r \rangle \simeq 1.00$. This indicates that using either code consistently for reconstructing $X_{\rm max}$ introduces a negligible uncertainty. In contrast, when reference showers are simulated with one code but reconstructed using templates from the other (right panel of Fig. 4), the mean values shift to $\mu \simeq +11.6 \pm 0.4$ and -12.3 ± 0.6 g/cm^2, the σ values ranges from 8.1 and 8.8 g/cm^2, while $\langle f_r \rangle < 1$ for showers simulated with CoREAS and reconstructed with ZHAireS, and $\langle f_r \rangle > 1$ in the reverse case, consistent with the larger field strengths predicted by CoREAS. This quantifies the intrinsic uncertainty introduced by models of radio emission in current simulation codes.

4. Conclusions

This study presents a detailed, reproducible comparison of the CoREAS and ZHAireS Monte Carlo codes for simulating radio emission from extensive air showers. Simulations were performed under matched conditions, same primaries, geomagnetic setup, atmospheric model, and closely matched $X_{\max}$, to isolate differences due to the codes themselves. A good agreement on the predictions of both codes is found. Across the 30 – 80 MHz band, electric field differences remain within 5% with ZHAireS systematically predicting lower signals than CoREAS. At higher frequencies (above $\sim$ 100 MHz), discrepancies grow due to sensitivity of coherence to the fine details of air shower modelling. Energy fluence maps and total radiation energy predictions agree within $\lesssim$ 10%. Using a simplified $X_{\max}$ reconstruction method, the added uncertainty due to the simulation code itself was found to be $\lesssim 12\,\mathrm{g/cm^2}$. Determining the source of these differences is challenging. CoREAS and ZHAireS use different approximations for energy-loss modeling and low-energy (below a few hundred GeV) hadronic interactions, and also employ distinct thinning algorithms, despite attempts to align their performance through parameter tuning. Isolating these effects would require significant changes to both codes, which is beyond the scope of this work.

Acknowledgments: María de Maeztu grant CEX2023-001318-M funded by MICIU/AEI /10.13039/501100011033; Xunta de Galicia, Spain (CIGUS Network of Research Centers and Consolidación 2021 GRC GI-2033 ED431C-2021/22 and 2022 ED431F-2022/15); Feder Funds; Ministerio de Ciencia, Innovación y Universidades/Agencia Estatal de Investigación, Spain (PID2022-140510NB-I00, PCI2023-145952-2); and European Union ERDF.

References

[1] **Pierre Auger** Collaboration, A. Aab *et al. Phys. Rev. Lett.* **116** no. 24, (2016) 241101.
[2] A. Corstanje *et al. Phys. Rev. D* **103** no. 10, (2021) 102006.
[3] **Pierre Auger** Collaboration, A. Abdul Halim *et al. Phys. Rev. Lett.* **132** no. 2, (2024) 021001.
[4] M. Gottowik, C. Glaser, T. Huege, and J. Rautenberg *Astropart. Phys.* **103** (2018) 87–93.
[5] C. S. Cruz Sanchez *et al. arXiv:2505.08920* .
[6] T. Huege, M. Ludwig, and C. W. James *AIP Conf. Proc.* **1535** no. 1, (2013) 128.
[7] D. Heck, J. Knapp, J. Capdevielle, G. Schatz, and T. Thouw, "Corsika: A monte carlo code to simulate extensive air showers." Fzka report 6019, forschungszentrum karlsruhe (1998).
[8] C. W. James *AIP Conf. Proc.* **1535** no. 1, (2013) 152.
[9] J. Gladstone and J. Dale *Philosophical Transactions of the Royal Society of London* **153** (1863) 317–343.
[10] J. Alvarez-Muniz, W. R. Carvalho, Jr., and E. Zas *Astropart. Phys.* **35** (2012) 325–341.
[11] S. J. Sciutto, "The AIRES system for air shower simulations: An Update," in *27th International Cosmic Ray Conference*. 6, 2001. arXiv:astro-ph/0106044.
[12] E. Zas, F. Halzen, and T. Stanev *Phys. Rev. D* **45** (1992) 362–376.
[13] S. Ostapchenko *Phys. Rev. D* **83** (2011) 014018.
[14] J. Ammerman-Yebra, J. Alvarez-Muñiz, and E. Zas *JCAP* **08** (2023) 015.
[15] C. Glaser, M. Erdmann, J. R. Hörandel, T. Huege, and J. Schulz *JCAP* **09** (2016) 024.
[16] S. Buitink *et al. Phys. Rev. D* **90** no. 8, (2014) 082003.
[17] W. R. Carvalho and J. Alvarez-Muñiz *Astroparticle Physics* **109** (2019) 41–49.
[18] S. Buitink *et al. Nature* **531** (2016) 70.
[19] **Pierre Auger** Collaboration, A. Abdul Halim *et al. Phys. Rev. D* **109** no. 2, (2024) 022002.
[20] P. A. Bezyazeekov *et al. Phys. Rev. D* **97** no. 12, (2018) 122004.